WATER RESOURCES RESEARCH, VOL. 49, 2975–2986, doi:10.1002/wrcr.20198, 2013

Temporal variability of exchange between groundwater and surface water based on high-frequency direct measurements of seepage at the sediment-water interface

Donald O. Rosenberry,[1] Richard W. Sheibley,[2] Stephen E. Cox,[2] Frederic W. Simonds,[3] and David L. Naftz[4]

Received 5 September 2012; revised 13 March 2013; accepted 14 March 2013; published 31 May 2013.

[1] Seepage at the sediment-water interface in several lakes, a large river, and an estuary exhibits substantial temporal variability when measured with temporal resolution of 1 min or less. Already substantial seepage rates changed by 7% and 16% in response to relatively small rain events at two lakes in the northeastern USA, but did not change in response to two larger rain events at a lake in Minnesota. However, seepage at that same Minnesota lake changed by 10% each day in response to withdrawals from evapotranspiration. Seepage increased by more than an order of magnitude when a seiche occurred in the Great Salt Lake, Utah. Near the head of a fjord in Puget Sound, Washington, seepage in the intertidal zone varied greatly from -115 to $+217$ cm d^{-1} in response to advancing and retreating tides when the time-averaged seepage was upward at $+43$ cm d^{-1}. At all locations, seepage variability increased by one to several orders of magnitude in response to wind and associated waves. Net seepage remained unchanged by wind unless wind also induced a lake seiche. These examples from sites distributed across a broad geographic region indicate that temporal variability in seepage in response to common hydrological events is much larger than previously realized. At most locations, seepage responded within minutes to changes in surface-water stage and within minutes to hours to groundwater recharge associated with rainfall. Likely implications of this dynamism include effects on water residence time, geochemical transformations, and ecological conditions at and near the sediment-water interface.

Citation: Rosenberry, D. O., R. W. Sheibley, S. E. Cox, F. W. Simonds, and D. L. Naftz (2013), Temporal variability of exchange between groundwater and surface water based on high-frequency direct measurements of seepage at the sediment-water interface, *Water Resour. Res.*, *49*, 2975–2986, doi:10.1002/wrcr.20198.

1. Introduction

[2] Flow across the sediment-water interface is substantially heterogeneous in most lakes, wetlands, streams, rivers, and estuaries. Many studies have addressed and quantified spatial heterogeneity, primarily to scale flux measured on the order of square meters to a river reach or shoreline segment or an entire lake [e.g., *Belanger and Kirkner*, 1994; *Burnett et al*., 2006; *Craig*, 2005; *Genereux et al*., 2008; *Kaser et al*., 2009; *Keery et al*., 2007; *Kikuchi et al*., 2012; *Mitchell et al*., 2008; *Rosenberry and Pitlick*, 2009b; *Rosenberry et al*., 2012; *Schmidt et al*., 2007; *Schneider et al*., 2005; *Simpkins*, 2006; *Stieglitz et al*., 2008]. Quantifying temporal heterogeneity is far less common, especially in lentic settings. A few studies have related seepage exchange in lakes to processes ranging from lake seiche [*Taniguchi and Fukuo*, 1996] to thunderstorms [*Rosenberry and Morin*, 2004] to seasonal changes in hydraulic gradients [*Schneider et al*., 2005]. Several studies in rivers have investigated temporal variability in hyporheic exchange driven by processes such as seasonal or event-driven changes in hydraulic gradients [e.g., *Doppler et al*., 2007; *Essaid et al*., 2006; *Keery et al*., 2007; *Kikuchi et al*., 2012; *Storey et al*., 2003], changing sediment properties [*Briggs et al*., 2012; *Doppler et al*., 2007; *Hatch et al*., 2010; *Kaser et al*., 2009; *Mutiti and Levy*, 2010; *Rosenberry and Healy*, 2012], or riverbed topography [*Hatch et al*., 2010; *Kaser et al*., 2009; *Rosenberry and Pitlick*, 2009b].

[3] With the exception of seepage response to tidal changes or lake seiche, most investigations of temporal variability in seepage have focused on changes in seepage over periods of weeks to months. However, it is reasonable to expect seepage to respond to processes that operate on scales of minutes to a day, such as rainfall events or evapotranspiration or floods. Changing seepage rates, and especially seepage direction, in response to these events can have a substantial effect on biota and biogeochemical processes [*McCutchan et al*., 2002; *Schuster et al*., 2003].

[1]U.S. Geological Survey, Lakewood, Colorado, USA.
[2]U.S. Geological Survey, Tacoma, Washington, USA.
[3]U.S. Geological Survey, Portland, Oregon, USA.
[4]U.S. Geological Survey, Salt Lake City, Utah, USA.

Corresponding author: D. O. Rosenberry, U.S. Geological Survey, M.S. 413, Bldg. 53, DFC, Lakewood, CO 80225, USA. (rosenber@usgs.gov)

0043-1397/13/10.1002/wrcr.20198

[4] Most studies that have investigated seepage on shorter time scales have measured seepage indirectly, using methods that either have a relatively long time-integration period or that may not relate well to seepage on short time periods. Seepage rates based on diurnal variability of temperature require a day or more of data and have a time-integration factor of about a day, although rapidly evolving technology and analytical approaches are greatly decreasing that time constant [*Lautz*, 2012]. Tracer-based measurements are dependent on the travel time between the tracer release and measurement points, and provide bulk exchange at a stream-reach scale. Measuring hydraulic gradient as a surrogate for seepage works well in many settings but may be misleading over short periods if the hydraulic properties are changing over time or if flow paths are not aligned with the axis of the well screen and sediment bed [*Kaser et al*., 2009; *Lautz*, 2010; *Rosenberry et al*., 2012].

[5] Direct measurement of exchange between groundwater and surface water is typically achieved using a manually operated seepage meter. A seepage-meter measurement integrates temporal variability over the duration that a seepage bag is attached to a cylinder that isolates a portion of the sediment-water interface through which seepage occurs. Bag-attachment time depends primarily on bag size and the seepage rate and can range from minutes to a day or more. Because the sensor is prone to operator error, investigators usually make multiple measurements and statistically summarize the results, extending the integration time to hours or days. Unless a study design dictates repeat measurements over the course of weeks or more, temporal variability is largely ignored for most studies that incorporate seepage meters.

[6] Integration time can be greatly shortened, however, by replacing the seepage bag with a flowmeter. Here we provide examples of seepage variability in response to common environmental influences (e.g., rain, wind, evapotranspiration) on temporal scales ranging from seconds to days. Results are based on direct measurements from a seepage meter capable of providing data with integration times ranging from seconds to minutes. We then discuss the likely importance of transience at these short-temporal scales.

2. Methods

[7] The half-barrel seepage meter [*Lee*, 1977] is perhaps the only device that provides a direct measurement of flow across the sediment-water interface. Amazingly inexpensive and simple in design, the device can provide accurate and repeatable data provided sources of error are recognized and addressed [*Rosenberry et al*., 2008]. Measurements made with this device are integrated over periods determined largely by the seepage rate. Fast seepage can be measured on the order of minutes whereas slow seepage can take days for a single measurement. Automated seepage meters were developed in the early 1990s when heat-pulse sensors, originally designed as sap-flow sensors for use in trees, were adopted for use with a seepage cylinder [*Taniguchi and Fukuo*, 1993]. Several other types of flowmeter have since been coupled with a seepage cylinder to make unattended seepage measurements on short time intervals [*Fritz et al*., 2009; *Krupa et al*., 1998; *Menheer*, 2004; *Paulsen et al*., 2001; *Rosenberry and Morin*, 2004; *Sholkovitz et al*., 2003; *Smith et al*., 2003; *Tryon et al*., 2001].

[8] Data presented here were collected with an electromagnetic flowmeter, originally developed for measuring fluid velocities in vertical boreholes [*Molz and Young*, 1993], connected to a seepage cylinder and referred to as an electromagnetic seepage meter (ESM) [*Rosenberry and Morin*, 2004]. This device was chosen because: (1) it has a low measurement threshold of 10 ml min^{-1}; (2) measurable flow rates span 3 orders of magnitude; (3) it has a relatively large cross-sectional diameter of 13 mm, generating very small head loss; and (4) it has no parts that extend into the flow field. With the 0.25 m^2 area covered by a standard half-barrel seepage cylinder, the minimum detectable seepage velocity is 5.6 cm d^{-1} [*Rosenberry and Morin*, 2004]. In locations where seepage rates were too slow to be measured by the flowmeter, the measured surface area was increased by ganging seepage cylinders to provide greater flow volume [*Rosenberry*, 2005] (Figure 1). With flow from four standard half barrels all routed to a single flowmeter, the minimum detectable seepage velocity is 1.4 cm d^{-1}. Standard deviation of 1 min averages of 5 s scan intervals is 0.56 cm d^{-1}. Standard deviation of 1 min output determined over 12 h at a constant seepage rate is 0.35 cm d^{-1}.

[9] The ESM shown in Figure 1 has four seepage cylinders (three regular half barrels and one low-profile cylinder) all routing flow to the electromagnetic flowmeter that is situated inside a vented shelter to reduce effects of currents and waves that otherwise might corrupt sensor output. A cable extends from the flowmeter to a signal processor that provides output to a digital data logger. A 100 amp h deep-cycle marine battery can power the system for about 1.5–2 days. A *Y*-valve is used to direct flow either to the electromagnetic flowmeter or to a separate shelter that houses a standard seepage-meter bag. For every installation, flow is routed to the seepage bag one to several times a day for a period long enough to make a bag measurement of the seepage rate. This provides confirmation that the ESM is performing as designed and also allows concurrent zero-flow measurements by the ESM, which are used to correct small amounts of drift in sensor output. A minimum water depth of about 0.2 m is required for submergence of the seepage cylinders and the electromagnetic flowmeter.

3. Study Sites

[10] Examples of high-temporal resolution seepage measurements are presented from six locations across the contiguous United States (Figure 2). Automated seepage meters were installed in freshwater lakes in Minnesota, New Hampshire, and Massachusetts; in a fjord in northwestern Washington; in a large river in northeastern Washington; and in a large, hypersaline lake in Utah.

[11] Shingobee Lake is a 66 ha lake in northern Minnesota surrounded by a mixed deciduous-hardwood forest. Situated low in the landscape, it receives groundwater discharge via springs and seeps distributed along the entire shoreline [*Rosenberry et al*., 2000]. Mirror Lake is a 10 ha pond in the southern White Mountains, New Hampshire. The lake has three stream inlets and an outlet, but loses more water on an annual basis via seepage to groundwater

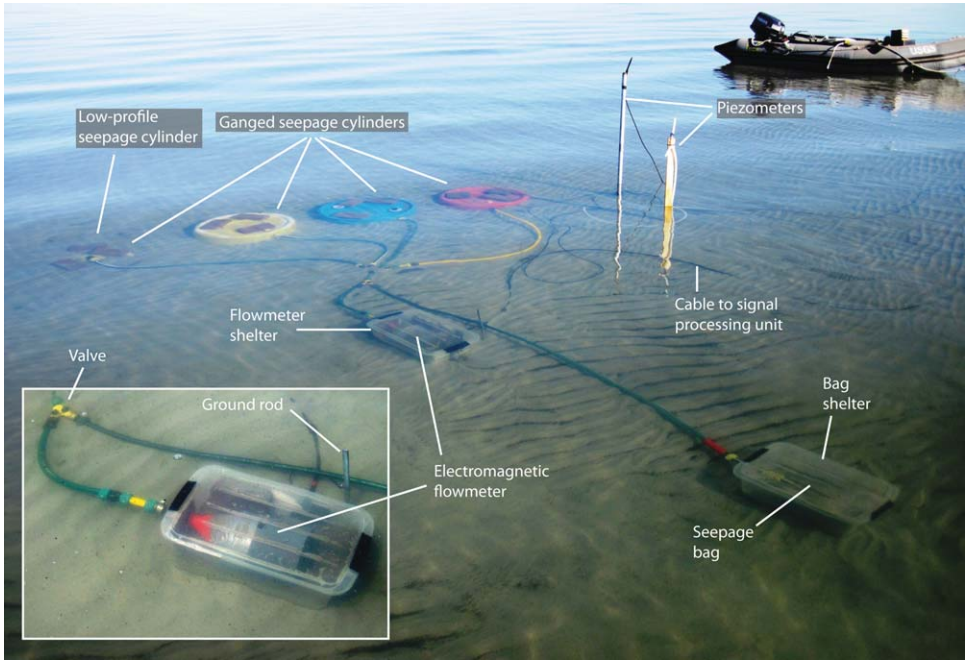

Figure 1. Automated seepage-meter installation in Great Salt Lake, Utah. Inset photograph shows close view of electromagnetic flowmeter situated inside a shelter to minimize effects from currents and waves. Also visible in the inset is a flow valve that routes water either to the electromagnetic flowmeter or to a seepage bag and shelter outside of the image but visible in the larger image.

than through the surface-water outlet [*Rosenberry et al*., 1999]. Ashumet Pond is an 88 ha lake situated near the center of Cape Cod, Massachusetts, and is a groundwater-flow-through kettle pond [*McCobb et al*., 2003]. The lake has no surface-water exchange; it receives groundwater discharge along the western and northern shorelines and loses water to groundwater along the eastern and southern shorelines. Hood Canal is a fjord in Puget Sound, northwestern Washington [*Simonds et al*., 2008]. Lynch Cove, situated at the head of Hood Canal, receives fresh water from several streams as well as substantial amounts of groundwater discharge along portions of the shoreline. The Columbia River is one of the largest rivers in North America. The reach between the USA-Canada border and Roosevelt Reservoir in northeastern Washington is subject to large changes in stage and discharge resulting from spring snowmelt, variable releases from dams located up-river, and changes in stage in Roosevelt Reservoir of tens of meters [*U.S. Geological Survey*, 2013]. Great Salt Lake, Utah, is a large, shallow, hypersaline lake that during data collection in 2010 was about 52 km wide and 120 km long with a maximum depth of about 8.5 m. During the time of data collection, lake water was about 4 times the salinity of sea water with a salinity of 143 parts per thousand. The lake receives freshwater discharge from several rivers as well as from groundwater. The study area in the southeastern corner of the lake was chosen because of concerns regarding the potential for selenium to enter the lake via groundwater discharge.

Figure 2. Study-area locations.

3.1. Response of Seepage to Rainfall

[12] Rainfall of sufficient magnitude to recharge groundwater should cause near-shore seepage rates to change [*Winter*, 1983], although few studies have documented this response with direct measurements. Three examples from midsummer are presented here to demonstrate the range of changes that can occur in response to relatively small and common rainfall events. The most intuitive of the three examples is from Ashumet Pond, Massachusetts, where seepage was measured 1.5 m from shore every 5 s and averaged over 1 min periods. Seepage was upward and fast, declining slowly from about 53 to about 51 cm d^{-1}, prior to 4.0 mm of rain that fell between 17:30 and 21:30 on 14 July (Figure 3a). Seepage continued to decline at a rate of 0.6 cm d^{-1} h^{-1} during the first 3.5 h of rainfall, and then began to increase. Seepage increased from 48 to a maximum rate of 55.5 cm d^{-1} at 22:45, 1.25 h after rainfall ended. These data demonstrate a delayed response in seepage caused by the time it took for rain falling on land near the lakeshore to infiltrate unsaturated sediments, reach the

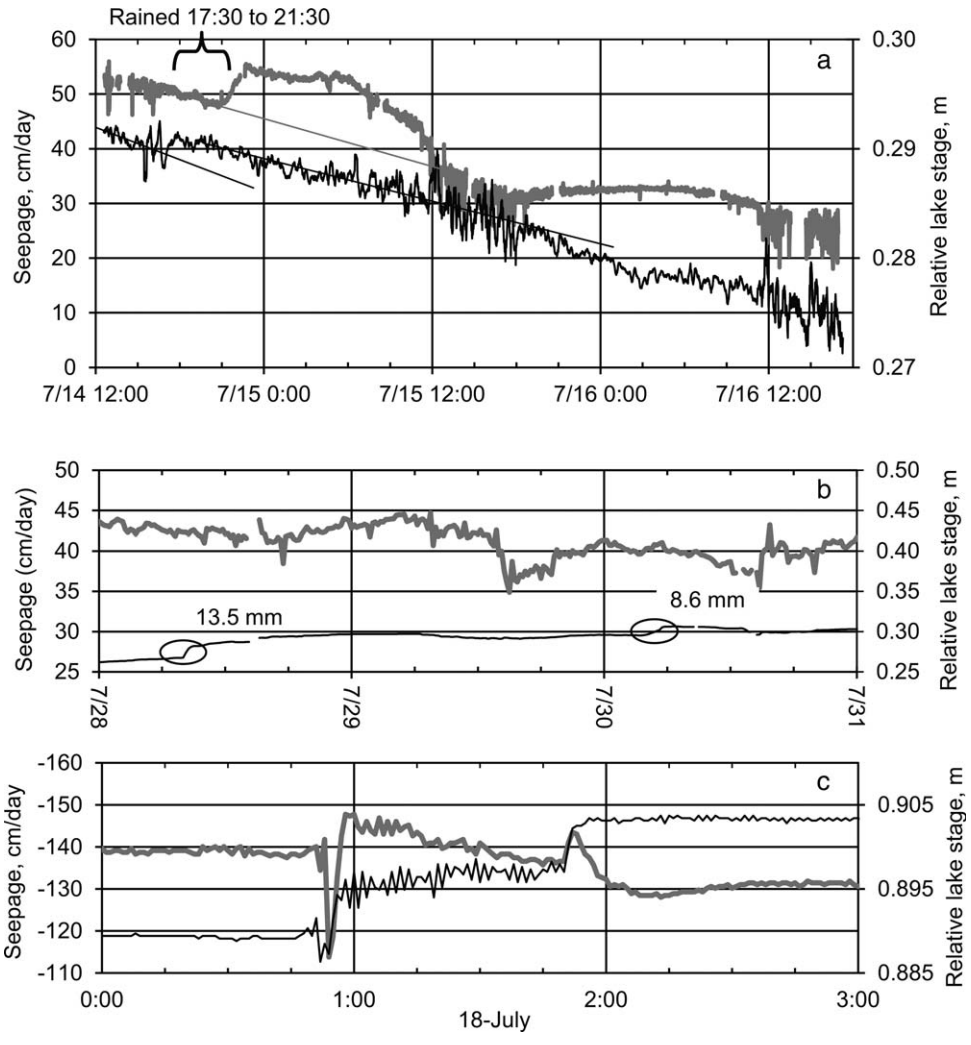

Figure 3. Seepage response (thick gray line) and lake-stage response (thin black line) to rainfall at (a) Ashumet Pond, (b) Shingobee Lake, (c) Mirror Lake. Circles in Figure 3a are discrete manual seepage measurements. Ovals in Figure 3b are periods of rainfall.

water table, and increase the hydraulic gradient in the groundwater adjacent to the shoreline of the lake. Lake stage, somewhat surprisingly, did not indicate an obvious stage rise in response to the 4 mm rainfall event (Figure 3a). Lake stage did rise 3 mm between 16:45 and 18:00 just prior to the onset of rainfall. This likely was due to an east to southeast wind that preceded rainfall and pushed water to the western side of the lake where the seepage meter was located. The other subtle response in lake stage was a reduction in the rate of lake-stage decline, from 0.50 mm h^{-1} prior to rainfall to 0.37 mm h^{-1} during and following rainfall, as shown by comparing the slopes of the two black dashed fitted lines. Lake-stage decline continued at approximately the same, slightly reduced rate until about 12:00 the following day. The increased seepage rate also appears to have returned to normal at about 12:00 the following day, based on extension of the rate of decline in seepage that occurred prior to rainfall (gray dashed line) (Figure 3a).

[13] Other interesting responses also are evident in the seepage and lake-stage records. Greater noise in both the seepage and lake-stage data during the afternoons of 14, 15, and 16 July was due to increased wind between about noon and about 18:00 each day. The cause of the slight increase then decrease in seepage that occurred from about 18:00 on 15 July to about 12:00 on 16 July is unknown.

[14] Similar seepage rates were measured at Shingobee Lake in north-central Minnesota during a 3 day period when more substantial rainfalls of 13.5 and 8.6 mm occurred (Figure 3b). Prior to rainfall, seepage at a lakebed area identified as a spring ranged from 42 to 44 cm d^{-1}. Lake stage rose 18 mm in response to a 13.5 mm rain on 28 July and 11 mm in response to an 8.6 mm rain on 30 July, and there was no obvious change in measured seepage rate. These data indicate the controlling hydraulic gradient that governed seepage at this location was not influenced by changes in lake stage. It is also possible that the seepage meter was positioned beyond the influence of flow paths affected by groundwater recharge focused in the near-shore margins of the lake.

[15] Perhaps the most interesting, and somewhat counterintuitive, seepage response to rainfall was presented in *Rosenberry and Morin* [2004] when they recorded seepage

during and following a thunderstorm that occurred shortly after midnight (Figure 3c). Seepage was downward, very fast, and steady prior to rainfall that began at 00:45 on 18 July. During the storm, Mirror Lake stage rose 14 mm in response to 16 mm of rainfall. Prior to the first pulse of rainfall, a wind gust piled water against the north (opposite) shore of the lake, causing a decline in lake stage at the measurement location along the southern shoreline. This 3 mm reduction in lake stage decreased the downward hydraulic gradient, decreasing seepage by 18%, from −139 to −114 cm d^{-1}. Once rain began, lake stage began to rise, increasing the vertical hydraulic gradient and causing a rapid increase in seepage rate, from −113 to −148 cm d^{-1}. The counterintuitive portion of the data begins at about 01:00 when lake stage continued to increase but downward seepage began to decrease. This likely was the result of recharge from rainfall infiltrating the unsaturated zone and reaching the water table adjacent to the lake. Assuming a porosity of about 0.3 for the approximately 0.5 m thick unsaturated sandy sediments, water-table rise would be larger than lake-stage rise, reducing the hydraulic gradient and causing a reduction in seepage.

[16] This sequence of events (minus the gust front and seiche) was repeated at 01:50, when rainfall intensity increased. Seepage decrease associated with the second rainfall pulse was more immediate and pronounced, indicating that groundwater recharge was more efficient during the latter portion of the thunderstorm. Lake stage and seepage rate both stabilized at new values within 15 min of passage of the thunderstorm.

[17] Seepage responded to local hydraulic gradients at two of these three sites where sediments were sandy and organic soils were thin. The response was nearly instantaneous at the Mirror Lake site (Figure 3c), but lagged the rainfall event at Ashumet Pond (Figure 3a). This indicates that the unsaturated sediments were either thicker or drier at the onset of rainfall at the Ashumet Pond site relative to the Mirror Lake site. At Shingobee Lake (Figure 3b), the lack of seepage response to rainfall indicates that either hydraulic head adjacent to the lake rose the same as the lake stage, or that seepage rate was controlled by larger-scale hydraulic gradients that were unaffected by small changes in hydraulic gradient at and near the lakebed.

3.2. Response of Seepage to Waves

[18] The effect of waves is evident in Figure 3a where seepage at Ashumet Pond is much more variable during the afternoons of 14, 15, and 16 July. Standard deviations during the windy hours of 12:00 to 18:00 were 1.3, 2.5, and 2.4 cm d^{-1} for 14, 15, and 16 July, respectively. Standard deviation of seepage during the calm night-time hours between midnight and 06:00 on 15 and 16 July was only 0.6 and 0.3, respectively, half to a tenth as large as during the afternoons.

[19] The data from Ashumet Pond were based on 1 min averages of sensor scans made every 5 s. Another dataset from Ashumet Pond, collected 80 m southwest of the previously described study location, was based on 1 s scans that were averaged every 15 s. This seepage meter was installed 10 m from shore so that the top of the cylinder was submerged about 10 cm beneath the water surface. Although wave amplitudes that afternoon were perhaps 1–3 cm in response to a pedestrian 2–3 m s^{-1} wind speed, seepage rates ranged from +293 to −342 cm d^{-1} (Figure 4). The average of 300 measurements made over 75 min was 4.3 cm d^{-1}, similar to the 3.4 cm d^{-1} average of two manual measurements made during the same time at an adjacent seepage meter.

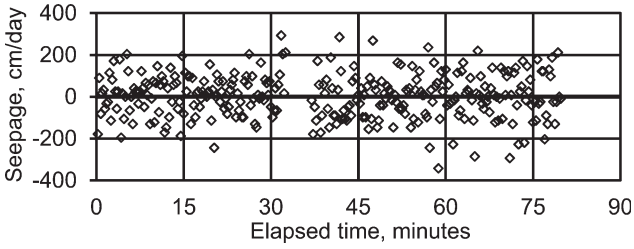

Figure 4. Seepage averaged over 15 s intervals at Ashumet Pond.

[20] These data indicate that water routinely flows across the sediment–water interface in response to passing waves of unremarkable size. Some of the instantaneous seepage rates are very large, suggesting that flow within the porous media likely is turbulent during windier times. Because force associated with turbulent flow is proportional to the square of velocity, some wave-generated seepage is likely able to transport sediment [*Turner and Masselink*, 1998]. This has been documented for upward seepage in particular [*Rosenberry and Pitlick*, 2009a; *Turner and Masselink*, 1998].

3.3. Response of Seepage to Evapotranspiration

[21] Seepage recorded at 1 min resolution over a 9 day period at Shingobee Lake showed substantial diurnal variability (Figure 5a) with seepage increasing during nighttime hours and decreasing during daytime hours. Seepage rate varied over a range of 3–5 cm d^{-1} during most days. Maximum seepage generally occurred between 04:15 and 06:30; minimum seepage generally occurred between 15:00 and 19:00. This response is similar to water-level changes that commonly occur in shallow monitoring wells as a result of evapotranspiration [e.g., *White*, 1932]. Curiously, this is the same location where a lack of seepage response to rainfall was observed (Figure 3b) and the rain events on July 28 and July 30, mentioned earlier, are visible in the lake-stage record (Figure 5a). (The lake-stage perturbation on 2–3 August was not related to rainfall and the cause of that aberration is unknown.)

[22] Seepage cylinders were located within 1–2 m of the shoreline where vegetation growing on peat was tall and dense; therefore, it is understandable that evapotranspiration might have an effect on seepage rate. There was no discernible diurnal signal in hydraulic gradient based on piezometers installed in the lakebed adjacent to the seepage cylinder and screened either 0.5 or 1.0 m beneath the bed. There was, however, a remarkable correlation between the daily maximum value of the mass-transfer product, which is directly correlated with evapotranspiration in wet environments, and the nadir in the diurnal pattern in seepage rate (Figure 5b). The mass-transfer product is based on vapor-pressure and wind-speed data collected from a raft deployed at the center of Shingobee Lake; data are, therefore, representative of conditions over and adjacent to the

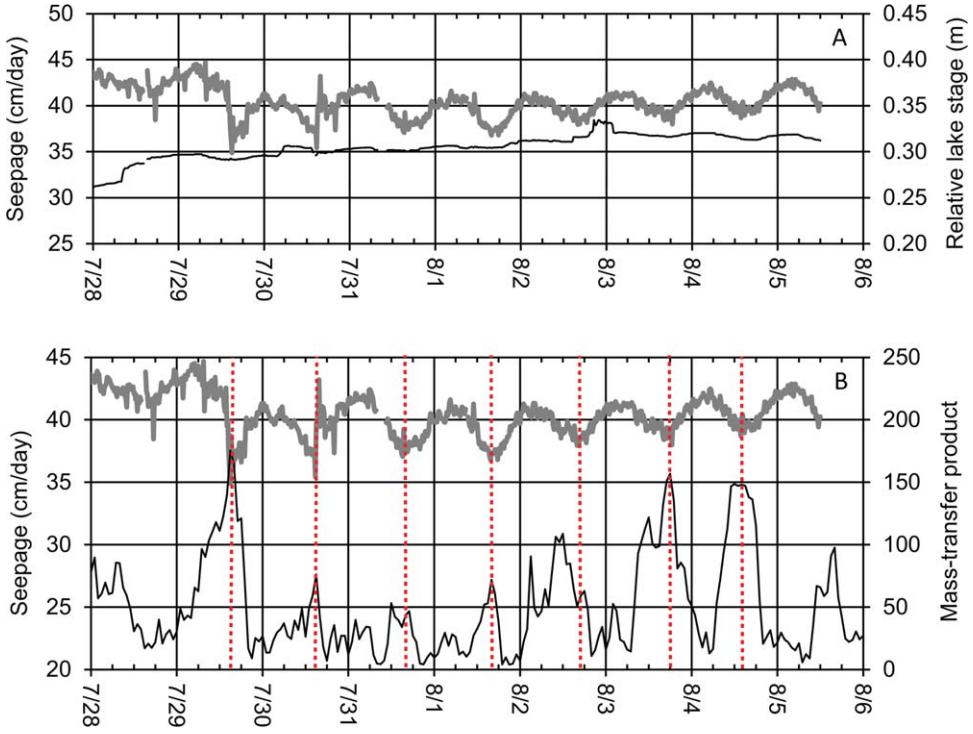

Figure 5. (a) Seepage (bold) and relative lake stage (thin) at Shingobee Lake (b) Seepage (bold) and the mass-transfer product (thin line) with dotted red lines placed at the daily nadir in seepage.

lake, including the area where seepage was measured. The inverse correlation shown in Figure 5b provides strong evidence that the diurnal response in seepage was directly linked to evapotranspiration by plants growing on the peat surface adjacent to the shoreline.

3.4. Response of Seepage to Lake Seiche

[23] Seepage was measured 0.6 km from shore near the southeastern corner of Great Salt Lake every 5 s and averages calculated each minute. Seepage was slow and averaged 0.75 cm d^{-1} over a nearly 3 day period (Figure 6a). Seepage was essentially zero during calm periods, but during windy periods seepage commonly ranged from -2 to $+3$ cm d^{-1}. Lake stage varied over a range of about 0.25 m during windy periods, which are visible as periods of enhanced noise in the lake-stage data (Figure 6a). Lake stage varied by less than 0.1 m during calm periods. Seepage was unrelated to lake stage except during the onset of windy weather, which often initiated upward seepage.

[24] The most prominent feature of the Great Salt Lake dataset was the lake-stage and seepage response to a typical thunderstorm that passed over the study site just prior to noon on 19 August (Figure 6b). Wind speed increased that day just after 09:00 on a typically sunny, calm morning (Figure 6c), well before the advance of the thunderstorm. The onset of a light wind caused seepage to increase from about 0 to about $+3.5$ cm d^{-1} but by 10:30 seepage had returned to an average value of 0 (Figure 6b). Wind increased substantially just prior to 11:00 with a sustained speed of 12.5 m s^{-1} and gusts of 15 m s^{-1} by 11:15. Lake stage rose 0.35 m from 10:45 to 11:30. Elevated lake stage reversed the hydraulic gradient and seepage direction reversed accordingly, with downward seepage of about -10 cm d^{-1} and a maximum downward seepage rate of -15.2 cm d^{-1} at 11:28. Maximum downward seepage was essentially coincident with maximum lake-stage values of 0.62 m at 11:26 and 0.66 m at 11:30. A west wind became an east wind at about noon (Figure 6c). Lake stage rapidly declined more than 0.5 m in response to the wind shift, from 0.66 m at 11:30 to 0.14 m at 12:31. As lake stage declined, the downward hydraulic gradient and downward seepage decreased until seepage returned to essentially 0 at 12:35. From 12:35 until 14:05, lake stage rose and then fell to a new low value of 0.08 m. During that 1.5 h period when lowered lake stage resulted in large upward hydraulic gradients, seepage increased rapidly from 0 to an average of $+10.3$ cm d^{-1} with a maximum value of $+24.0$ cm d^{-1} at 12:49. From 14:05 to about 15:00, seepage decreased to a relatively stable average value of $+1.0$ cm d^{-1} in response to a rising lake stage and corresponding decreasing upward hydraulic gradient. Seepage continued at that rate until 16:30, when it abruptly returned to zero.

3.5. Response of Seepage to Tides

[25] Seepage measured in Lynch Cove of Puget Sound, Washington, showed little response to 3.5–5 m of tidal range when measured beyond the low-tide line [*Simonds et al.*, 2008]. However, seepage measured in the intertidal zone between low and high tide showed some very interesting temporal variability.

[26] The ESM was installed about 25 m from the extreme high-tide line on a steeply sloping cobble to gravel-bed beach. This portion of the bed was exposed during the daily low tide, interrupting seepage measurements for about 8 h each day. Seepage measurements resumed each day when the water level was sufficient to fully submerge the 1.5 m

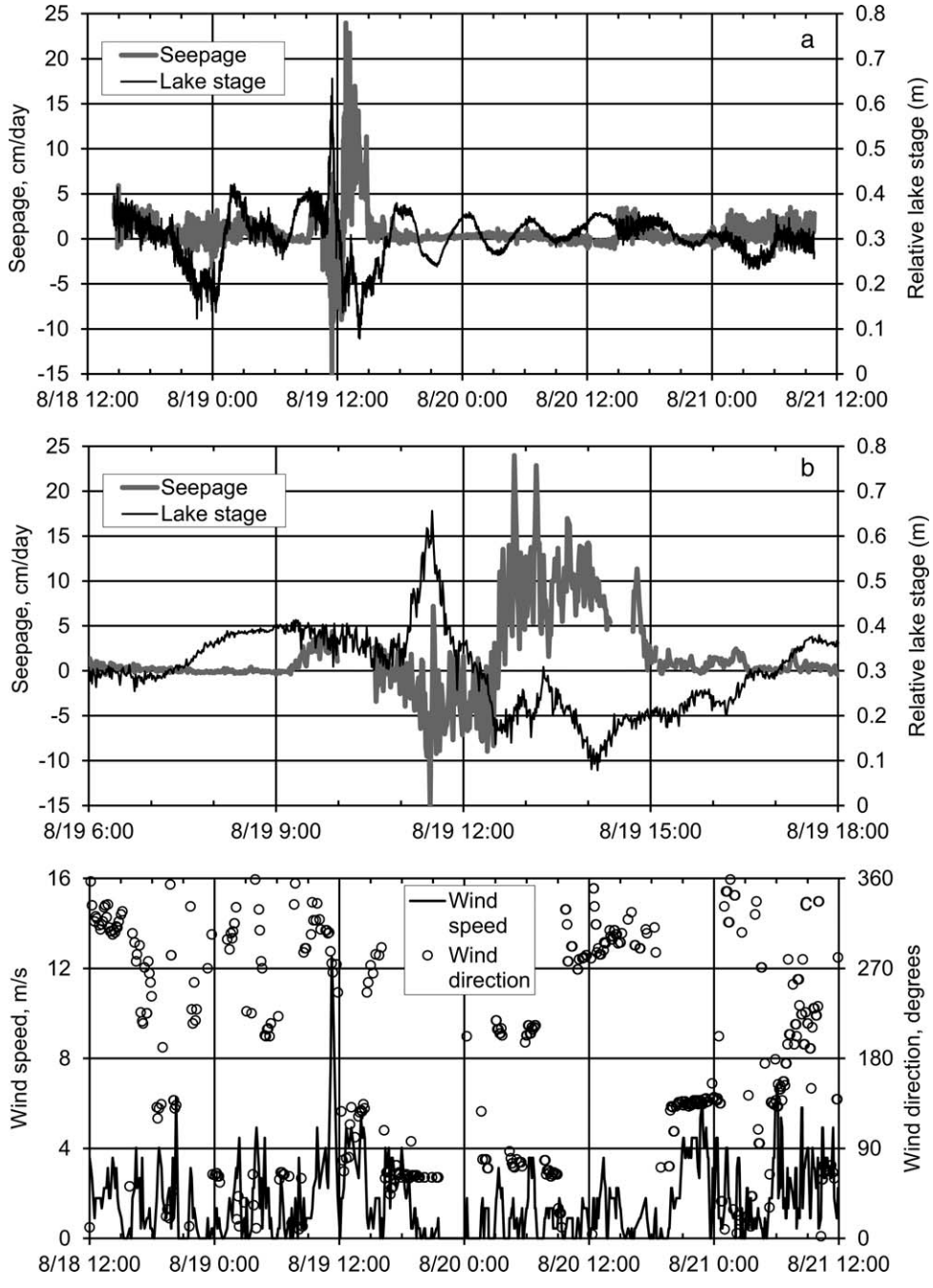

Figure 6. Seepage (gray line) and lake stage (black line) at Great Salt Lake. (a) Data collected over 3 day period. (b) Data collected during seiche event. (c) Wind speed and direction measured at Saltair Marina, 2.2 km to the southwest.

diameter seepage cylinder. During the times when the seepage cylinder was fully submerged and seepage could be measured, the average seepage was upward at +42.9 cm d^{-1} (Figure 7a).

[27] Seepage across the sediment-water interface was very fast and downward for the first 1–3 h after measurements began each day with the rising tide (Figure 7a). Water flowed downward into the bed sediments as the tide rose, the shoreline moved up the sloping bed beyond the ESM, and local downward hydraulic gradients were correspondingly and momentarily large. Initial seepage rates immediately following ESM inundation ranged from −115 to −217 cm d^{-1} during the 6 days of data shown in Figure 7a. Initial seepage rates undoubtedly were larger, but they were unmeasurable until water depth at the meter reached approximately 35 cm, sufficient to fully submerge the seepage cylinder. Downward seepage decreased rapidly as the tide continued to rise, and then reversed to become upward seepage, the reversal occurring usually 20–90 min before the transition from a rising to a falling tide. Upward seepage increased at the same rate of about 73 cm d^{-1} h^{-1}, ranging from 36 cm d^{-1} h^{-1} on June 8 to 107 cm d^{-1} h^{-1} on June 12 (Figure 7a).

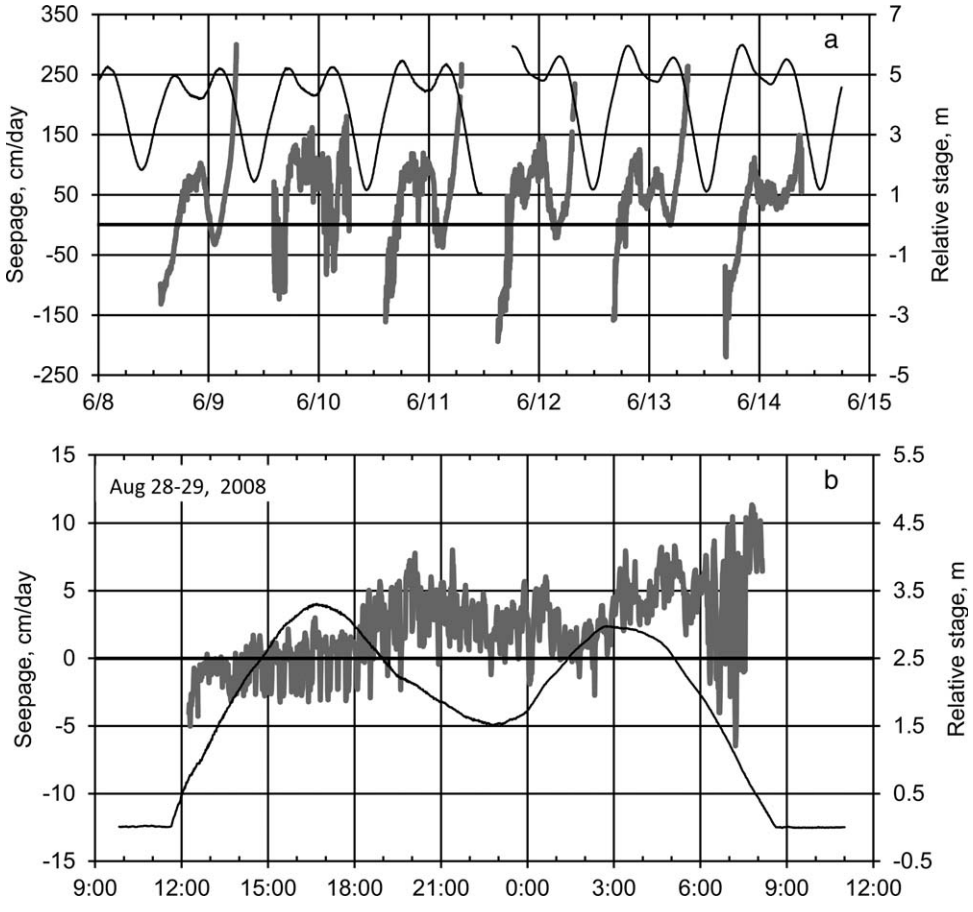

Figure 7. Seepage response (thick gray line) and surface-water stage (thin black line) at Hood Canal. (a) Steeply sloping intertidal site, (b) Gently sloping intertidal site.

[28] Increase in upward seepage either slowed or stopped as the tide fell toward the higher of the low-tide marks. Decrease in upward seepage occurred, sometimes suddenly, usually between 2 and 2.5 h after the first tidal apex. A more substantial decrease in upward seepage occurred soon after the beginning of stage rise to the second high tide. During five of six daily cycles, this larger decrease in upward seepage continued until seepage direction reversed to become downward seepage for several hours before becoming upward seepage again, usually just before the second high tide. Once the tide began falling rapidly toward the lowest daily tide, seepage increased rapidly until it reached maximum values ranging from +150 to +300 cm d^{-1}, at which point the seepage cylinder began to be exposed by the falling tide.

[29] This dynamic pattern of seepage response to changing tides is subdued in finer-grained sediments on a lower-gradient bed where the horizontal distance of the intertidal zone is substantially larger (Figure 7b). At this location closer to the head of the fjord, seepage measured in the intertidal zone averaged only +2.3 cm d^{-1}. Measurements made about 100 m from the high-tide line during a nearly 20 h period when the seepage cylinder was submerged showed temporal variability similar to that observed at the cobble-bed site, but it was substantially masked by wind-driven waves. Seepage at 12:15 was downward at −5 cm d^{-1} and gradually decreased to zero at about 15:00 to 18:00, approximately coincident with high tide (Figure 7b). Subsequent upward seepage ranged between 0 and +7 cm d^{-1} and then gradually decreased until the second high tide was reached, after which the upward seepage rate began to increase again. Seepage variability increased substantially from 06:00 to 07:30, indicating a period of stronger winds. Seepage continued to increase to a maximum value of 11.3 cm d^{-1} just prior to the seepage cylinder being exposed by the falling tide.

[30] These patterns in seepage response to tides indicate a complex and dynamic interface exists in the intertidal zone. Volumes of water and associated nutrients and chemicals that flow across the sediment-water interface each day are much larger than previously thought, resulting in a substantially larger mixing volume in the pore waters beneath the broad intertidal zone that covers over 4.6 km^2 of the bed of Lynch Cove [*Simonds et al*., 2008].

3.6. Seepage Response to Anthropogenic River-Stage Change

[31] Seepage measured 3–4 m from the shoreline of the Columbia River near Deadman's Eddy, 4 km downriver from the USA-Canada border, was downward and slow, ranging between −6.5 and −1.5 cm d^{-1} during early to midafternoon of September 27 (Figure 8). Seepage slowly decreased as day progressed to night and approached zero at 22:00. River stage, meanwhile, rose 0.1 m between noon

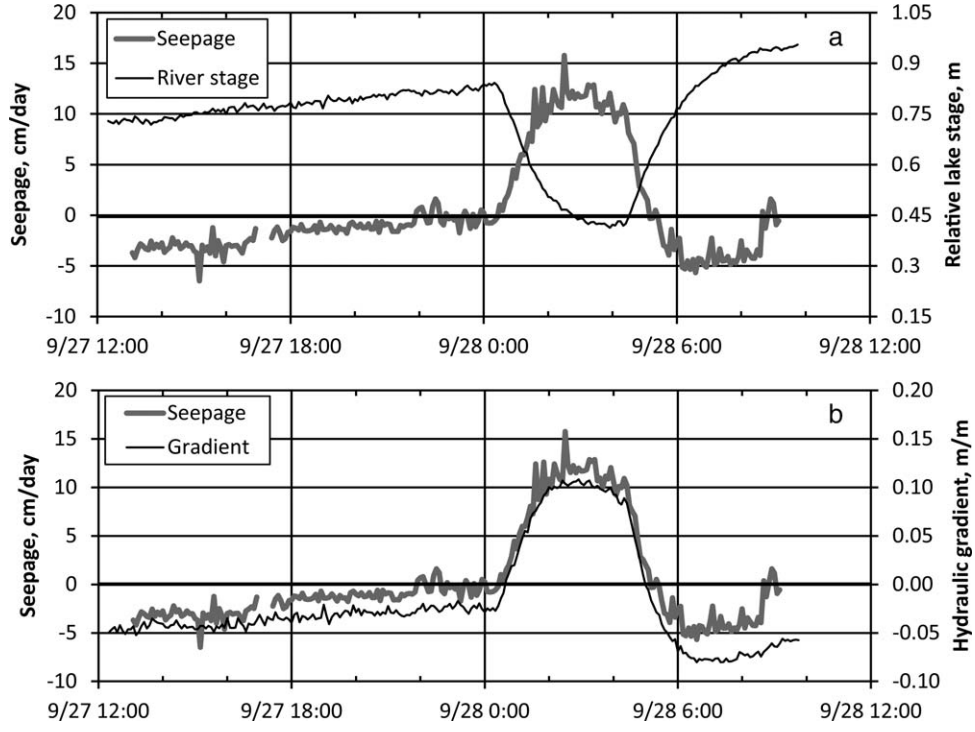

Figure 8. Seepage response to anthropogenic influence (river-stage change). (a) Seepage and relative Columbia River stage; (b) Seepage and hydraulic gradient between river surface and a nearby water-table monitoring well.

and midnight (Figure 8a) and a downward hydraulic gradient decreased slightly during the same period (Figure 8b). Conditions changed markedly shortly after midnight. Reduction in discharge from an up-river power-supply dam located on a tributary to the Columbia River in Canada caused river stage at the measurement site to decrease by about 0.4 m from 00:35 to 04:05. This caused a reversal in the hydraulic gradient, which reversed the seepage direction. Upward seepage increased from 0 to about + 12 cm d^{-1} with a maximum seepage rate of +15.8 cm d^{-1} occurring at 02:30. Upward seepage persisted for about 5 h until rising river stage caused the hydraulic gradient and seepage direction to reverse again. Downward seepage resumed at about 05:25. By 09:15, river stage had risen 0.5 m and reached the stage that would be predicted based on the trend in river stage from the previous day. Downward seepage increased to a maximum rate of −5 cm d^{-1}, slowly decreased and then suddenly decreased to essentially 0 at 08:45.

[32] Hydraulic gradient was determined on a horizontal axis based on comparing river stage with hydraulic head in a water table well located about 2 m from the river. Seepage and hydraulic gradient are nearly perfectly correlated, demonstrating the strong and instant response in seepage to near-shore hydraulic gradient in this sandy to bouldery setting (Figure 8b).

4. Discussion and Implications

[33] We often assume that temporal variability in exchange between groundwater and surface water is much smaller or less important than spatial variability. In some settings, where the bulk of the exchange is focused in discrete locations, such as springs or seeps, or in karstic settings [*Belanger and Kirkner*, 1994], that likely is true. In many other settings, however, we simply do not have enough information to make that determination.

[34] As indicated in the introduction, many investigators have documented seepage variability on scales of weeks to seasons. Several have measured variability in tidal settings with approximately hourly resolution. At least one study measured temporal variability in seepage with 30 min resolution over a 2 week period and found that seepage rate and direction responded primarily to changes in river stage [*Fritz et al*., 2009].

[35] Examples presented here indicate that temporal variability is much more substantial than previously realized. The relevance of this variability largely has yet to be determined, but some examples of relevance are fairly simple to surmise. The observation that groundwater recharge associated with rainfall causes seepage to increase is not surprising, but the immediacy and magnitude of the response may be. It is likely that few would have expected already large seepage rates to change so substantially in response to relatively small rainfall events. Seepage increased by 16% at Ashumet Pond following only 4 mm of rainfall. At Mirror Lake, already large rates of downward seepage increased by 10 cm d^{-1} (7%) in response to what likely was 6 mm of rain based on the lake-stage change. These changes in seepage were substantial and occurred within minutes (Mirror Lake) to a few hours (Ashumet Pond) of the onset of small amounts of rainfall. These flushing events likely are much more substantial during large rainfall events. Chemicals weakly adsorbed to sediments at or just above the water

table could easily be mobilized during these flushing events. This process could be enhanced in near-shore margins where unsaturated zones are thin and chemicals may be concentrated by evapotranspiration [*Winter*, 2003].

[36] But this dynamic and rapid response to rainfall does not occur everywhere. At Shingobee Lake, rainfalls of 8.6 and 13.5 mm resulted in no measurable change in seepage rate. One possible explanation posed earlier is that the ESM was not situated within the zone of influence associated with near-shore recharge events. Local-scale rainfall-driven recharge events that are focused at or near the shoreline should have the greatest influence on seepage fluxes closest to the shoreline [*McBride and Pfannkuch*, 1975; *Pfannkuch and Winter*, 1984], which is why seepage cylinders are usually positioned in shallow, near-shore margins to quantify these transient hydrological processes. It is possible that peat adjacent to the shoreline of the lake functioned as an extension of the lake. If the peat had very high porosity (likely), and the water table was virtually at land surface (this was the case), then rain that fell on the peat would cause a nearly identical change in hydraulic head in the peat compared to the rise in the adjacent lake surface. In this case, the seepage meter would be located tens of meters from the break in slope and associated focused recharge where the peat abuts the upland. There would be no change in local hydraulic gradient and no resulting change in measured seepage rate associated with focused groundwater-recharge because the ESM, even though positioned as close to the shoreline as possible, was removed from those near-shore processes.

[37] Although small to moderate rainfall did not affect seepage at Shingobee Lake, seepage varied by about 10% in response to evapotranspiration occurring at and landward of the shoreline. Seepage was upward and fast at this location because the lake is situated low in the landscape and serves as a drain at the end of a large hydrogeologic flow system. Therefore, evapotranspiration exerted a relatively minor influence on seepage at this location. However, in settings where hydraulic gradients and seepage rates are small, evapotranspiration could cause reversals in seepage direction on a daily basis. This could influence oxygen concentrations and chemistry in the substrate and alter the ecological conditions at this important ecotone. Diurnal changes in exchange between groundwater and surface water have been documented in several settings based on measurement of hydraulic gradient in wells situated adjacent to surface water [*Lott and Hunt*, 2001; *Simonds and Sinclair*, 2002; *Szilagyi et al*., 2008], but this may be the first time that diurnal changes in seepage have been documented with direct measurements. All the more interesting is that corresponding diurnal changes in vertical hydraulic gradients at piezometers located adjacent to the seepage meter did not occur at Shingobee Lake. The lack of change in vertical hydraulic gradients beneath the lakebed indicates that diurnal variability in seepage was due to changes in primarily horizontal flow at and near the shoreline. This also indicates that the influence of evapotranspiration occurring on the peat surface extends lakeward at least several meters beyond the shoreline.

[38] The effect of waves was evident in just about every dataset presented here. Close to the shoreline, wave height is amplified and instantaneous seepage rates become larger as a result. Data integrated over 15 s intervals at Ashumet Pond indicate wave-generated seepage rates are very large in sandy sediments 10 m from the shoreline. Seepage rates would be larger yet during storms. This could be relevant to rates of chemical transformations and water residence times. It also could indicate that processes attributed largely to diffusion may actually be driven to a greater extent by advection.

[39] Lake seiche is essentially a very large wave that operates on a much longer time scale. The several-hour seiche documented in Great Salt Lake was by far the largest influence on seepage measured during 4 days at Great Salt Lake. Seepage averaged 0.54 cm d^{-1} during the 3 day measurement period excluding the lake-seiche event. Even though the initial response of the lake seiche was to push lake water downward into the bed, the net effect of the lake seiche was an increase of the average seepage rate to +2.54 cm d^{-1}, nearly 4.5 times larger than during the rest of the period of data collection. And the maximum seepage rates were on the order of 25 cm d^{-1}. The purpose for making these measurements was to determine if, where, and to what extent, selenium is discharging to the lake [*Naftz et al*., 2008b]. If typical rates of seepage are assumed, selenium loading may be small. However, discharge of selenium may be episodic, and may occur primarily during these seiche events that generate rapid pulsing of groundwater discharge to the lake.

[40] Seiche events and associated groundwater pulses could also have implications with respect to the high levels of mercury in water and biota utilizing Great Salt Lake [*Naftz et al*., 2008a, 2011]. The observed sulphate-reducing conditions about 1 m below the sediment/water interface in these near-shore areas could increase methylation of inorganic forms of mercury and its corresponding flux to the lake during the observed groundwater pulses. Once in the lake water, the methylmercury could be subject to bioaccumulation in the brine shrimp population that thrives in the hypersaline waters and provides a critical food source to migratory waterfowl.

[41] These episodes of seiche-induced rapid seepage discharge would be difficult to document without automated measurements. Furthermore, the 0.5 m seiche event reported here was not exceptional. Only 1 day after the field campaign ended, a more substantial wind event caused a lake-stage change of 0.7 m at a USGS lake-stage gage 2.2 km southwest of the study location. Continuous data collected at that gaging station between 1 August 2010 and 1 August 2011 indicated 12 events with lake-stage changes of 0.5 m or more, the largest a change of 1.0 m.

[42] Blooms of toxic algae, periods of low dissolved oxygen, and fish-kill events instigated research on groundwater discharge in the intertidal zone of Lynch Cove at the head of Hood Canal in Puget Sound, Washington [*Simonds et al*., 2008; *Swarzenski et al*., 2007]. If nutrients were entering the fjord from leaking septic systems, the area of nutrient loading likely would occur in the intertidal area. Rates of exchange between pore water and surface water, and the degree of oxygenation in the pore water, would have a large effect on rates of nitrogen transformation and ultimately on the extent to which nutrients affect water in the fjord. Although reversals in seepage in response to tidally driven shoreline movement was not a surprise, the exceptionally

rapid seepage rates were. Large seepage rates continued for 6 or more hours after each tidal cycle, indicating that fluid exchange and rates of flushing were more substantial than previously thought. Stationary electrical resistivity surveys, continuous radon measurements, and automated seepage-meter data all proved useful in showing the temporal variability in groundwater discharge into this saline estuary [*Simonds et al*., 2008]. Taken together, these data provide an unprecedented level of temporal information on how distinct plumes of fresh water push seaward during outgoing tides and are then mixed with recirculated saline water during incoming tides. These transient conditions may be the main driver in controlling nutrient transformations and in mitigating rates of nutrient loading to this important estuary. The health of benthic organisms that live in the intertidal zone may also be closely tied to this process.

[43] Seepage at the Columbia River site was unremarkable during the daytime hours, the only surprise being that seepage was downward. In this deeply incised Columbia River gorge, and during the fall following senescence, it would be prudent to expect upward seepage. Without use of the ESM, the seepage reversal and substantial rates of groundwater discharge to the river during the night-time hours likely would have been completely missed. Manual seepage measurements in this remote location during night-time hours would be very difficult due to tricky river navigation in strong currents, darkness, and fog. Trace elements, including copper, are present in sometimes large concentrations in the pore water of these Columbia River sediments [*Paulson and Cox*, 2007]. This could pose a health risk to organisms that reside in interstitial pore spaces near the sediment-water interface and that are sensitive to these concentrations of trace elements. Large concentrations of metals in pore water could be construed as a smaller risk with downward seepage as determined during daytime measurements. Interpretation of risk could be completely different with the knowledge of night-time flow reversals and the substantial seepage rates that cause pore water to enter the river.

[44] Our limited understanding of temporal variability stems in part from the commonly held perception that seepage changes little over periods of a day or less. These data clearly indicate this is not the case in most settings. Data presented here also were not collected during extreme conditions, but instead represent short-term temporal variability during typical conditions. Exchanges almost certainly are much larger and more variable during extreme events. More work needs to be done to characterize this variability and the resulting effects on geochemical and biological processes at these shorter time scales.

[45] **Acknowledgments.** The authors thank Joshua Koch, Dallas Hudson, and Ryan Anderson (USGS), Elizabeth Kochevar (Colorado College), Eli Parkhurst (Colorado State University), and Seth Book (Mason County Public Health Department), all of whom provided valuable and greatly appreciated field assistance. Insightful reviews by Rebecca Schneider, Joshua F. Valder, and two anonymous reviewers substantially improved the manuscript. Partial funding for work on Great Salt Lake was provided by the Utah Department of Natural Resources/Division of Forestry, Fire, and State Lands.

References

Belanger, T. V., and R. A. Kirkner (1994), Groundwater/surface water interaction in a Florida augmentation lake, *Lake Reserv. Manage.*, *8*(2), 165–174.

Briggs, M. A., L. K. Lautz, J. M. McKenzie, R. P. Gordon, and D. K. Hare (2012), Using high-resolution distributed temperature sensing to quantify spatial and temporal variability in vertical hyporheic flux, *Water Resour. Res.*, *48*, W02527, doi:10.1029/2011WR011227.

Burnett, W. C., et al. (2006), Quantifying submarine groundwater discharge in the coastal zone via multiple methods, *Sci. Total Environ.*, *367*, 498–543.

Craig, A. L. (2005), Evaluation of spatial and temporal variation of groundwater discharge to streams, MSc thesis, 117 pp., Clemson Univ., Clemson, S. C.

Doppler, T., H.-J. H. Franssen, H.-P. Kaiser, U. Kuhlman, and F. Stauffer (2007), Field evidence of a dynamic leakage coefficient for modelling river–aquifer interactions, *J. Hydrol.*, *347*, 177–187.

Essaid, H. I., J. T. Wilson, and N. T. Baker (2006), Spatial and temporal variability in streambed fluxes, Leary Weber Ditch, Indiana, paper presented at Third Federal Interagency Hydrologic Modeling Conference, Joint Federal Interagency Conference, Subcommittee on Hydrology, Reno, Nev., 2–6 April 2006.

Fritz, B. G., D. P. Mendoza, and T. J. Gilmore (2009), Development of an electronic seepage chamber for extended use in a river, *Ground Water*, *47*(1), 136–140.

Genereux, D. P., S. Leahy, H. Mitasova, C. D. Kennedy, and D. R. Corbett (2008), Spatial and temporal variability of streambed hydraulic conductivity in West Bear Creek, North Carolina, USA, *J. Hydrol.*, *358*, 332–353.

Hatch, C. E., A. T. Fischer, C. R. Ruehl, and G. Stemler (2010), Spatial and temporal variations in streambed hydraulic conductivity quantified with time-series thermal methods, *J. Hydrol.*, *389*, 276–288.

Kaser, D. H., A. Binley, A. L. Heathwaite, and S. Krause (2009), Spatio-temporal variations of hyporheic flow in a riffle-step-pool sequence, *Hydrol. Process.*, *23*, 2138–2149.

Keery, J., A. Binley, N. Crook, and J. W. N. Smith (2007), Temporal and spatial variability of groundwater–surface water fluxes: Development and application of an analytical method using temperature time series, *J. Hydrol.*, *336*, 1–16.

Kikuchi, C. P., T. P. A. Ferré, and J. M. Welker (2012), Spatially telescoping measurements for improved characterization of ground water-surface water interactions, *J. Hydrol.*, *446–447*, 1–12.

Krupa, S. L., T. V. Belanger, H. H. Heck, J. T. Brock, and B. J. Jones (1998), Krupaseep–The next generation seepage meter, *J. Coast. Res.*, Special Issue (*26*), 210–213.

Lautz, L. K. (2010), Impacts of nonideal field conditions on vertical water velocity estimates from streambed temperature time series, *Water Resour. Res.*, *46*, W01509, doi:01510.1029/02009WR007917.

Lautz, L. K. (2012), Observing temporal patterns of vertical flux through streambed sediments using time-series analysis of temperature records, *J. Hydrol.*, *464–465*, 199–215.

Lee, D. R. (1977), A device for measuring seepage flux in lakes and estuaries, *Limnol. Oceanogr.*, *22*(1), 140–147.

Lott, R. B., and R. J. Hunt (2001), Estimating evapotranspiration in natural and constructed wetlands, *Wetlands*, *21*(4), 614–628.

McBride, M. S., and H. O. Pfannkuch (1975), The distribution of seepage within lakebeds, *U.S. Geol. Surv. J. Res.*, *3*(5), 505–512.

McCobb, T. D., D. R. LeBlanc, D. A. Walter, K. M. Hess, D. B. Kent, and R. L. Smith (2003), *Phosphorus in a ground-water contaminant plume discharging to Ashumet Pond, Cape Cod, Massachusetts, 1999*, Water-Resour. Invest. Rep. 02–4306, 69 pp., U.S. Geol. Surv., Northborough, Mass.

McCutchan Jr., J. H., J. F. Saunders III, W. M. Lewis Jr., and M. G. Hayden (2002), Effects of groundwater flux on open-channel estimates of stream metabolism, *Limnol. Oceanogr.*, *47*(1), 321–324.

Menheer, M. A. (2004), Development of a benthic-flux chamber for measurement of ground-water seepage and water sampling for mercury analysis at the sediment-water interface, Sci. Invest. Rep. 2004–5298, 14 pp., U.S. Geol. Surv., Reston, Va.

Mitchell, N., J. E. Nyquist, L. Toran, D. O. Rosenberry, and J. S. Mikochik (2008), Electrical resistivity as a tool for identifying geologic heterogeneities which control seepage at Mirror Lake, NH, paper presented at Symposium on the Application of Geophysics to Engineering and Environmental Problems, Environmental and Engineering Geophysical Society, Philadelphia, Penn., 6–10 April 2008.

Molz, F. J., and S. C. Young (1993), Development and application of borehole flowmeters for environmental assessment, *Log Anal.*, *1*, 13–23.

Mutiti, S., and J. Levy (2010), Using temperature modeling to investigate the temporal variability of riverbed hydraulic conductivity during storm events, *J. Hydrol.*, *388*, 321–334.

Naftz, D. L., C. Angeroth, T. Kenney, B. Waddell, S. Silva, N. Darnall, C. Perschon, and J. Whitehead (2008a), Anthropogenic influences on the input and biogeochemical cycling of nutrients and mercury in Great Salt Lake, Utah, USA, *Appl. Geochem.*, *23*, 1731–1744.

Naftz, D. L., W. P. Johnson, M. L. Freeman, K. Beisner, X. Diaz, and V. A. Cross (2008b), *Estimation of selenium loads entering the south arm of Great Salt Lake*, Utah, from May 2006 through March 2008, Sci. Invest. Rep. 2008–5069, 40 pp., U.S. Geol. Surv., Reston, Va.

Naftz, D. L., J. R. Cederberg, D. P. Krabbenhoft, K. R. Beisner, J. Whitehead, and J. Gardberg (2011), Diurnal trends in methylmercury concentration in a wetland adjacent to Great Salt Lake, Utah, USA, *Chem. Geol.*, *283*, 78–86.

Paulsen, R. J., C. F. Smith, D. O'Rourke, and T. Wong (2001), Development and evaluation of an ultrasonic ground water seepage meter, *Ground Water*, *39*(6), 904–911.

Paulson, A. J., and S. E. Cox (2007), Release of elements to natural water from sediments of Lake Roosevelt, Washington, USA, *Environ. Toxicol. Chem.*, *26*(12), 2550–2559.

Pfannkuch, H. O., and T. C. Winter (1984), Effect of Anisotropy and groundwater system geometry on seepage through lakebeds, 1. Analog and dimensional analysis, *J. Hydrol.*, *75*, 213–237.

Rosenberry, D. O., P. A. Bukaveckas, D. C. Buso, G. E. Likens, A. M. Shapiro, and T. C. Winter (1999), Migration of road salt to a small New Hampshire lake, *Water Air Soil Pollut.*, *109*, 179–206.

Rosenberry, D. O., R. G. Striegl, and D. C. Hudson (2000), Plants as indicators of focused ground water discharge to a northern Minnesota lake, *Ground Water*, *38*(2), 296–303.

Rosenberry, D. O., and R. H. Morin (2004), Use of an electromagnetic seepage meter to investigate temporal variability in lake seepage, *Ground Water*, *42*(1), 68–77.

Rosenberry, D. O. (2005), Integrating seepage heterogeneity with the use of ganged seepage meters, *Limnol. Oceanogr. Methods*, *3*, 131–142.

Rosenberry, D. O., J. W. LaBaugh, and R. J. Hunt (2008), Use of monitoring wells, portable piezometers, and seepage meters to quantify flow between surface water and ground water, in *Field techniques for estimating water fluxes between surface water and ground water* edited by D. O. Rosenberry and J. W. LaBaugh, pp. 39–70, U.S. Geol. Surv. Tech. and Methods 4-D2, Denver, Colo.

Rosenberry, D. O., and J. Pitlick (2009a), Effects of sediment transport and seepage direction on hydraulic properties at the sediment-water interface of hyporheic settings, *J. Hydrol.*, *373*, 377–391.

Rosenberry, D. O., and J. Pitlick (2009b), Local-scale spatial and temporal variability of seepage in a shallow gravel-bed river, *Hydrol. Process.*, *23*, 3306–3318.

Rosenberry, D. O., and R. W. Healy (2012), Influence of a thin veneer of low-hydraulic-conductivity sediment on modelled exchange between river water and groundwater in response to induced infiltration, *Hydrol. Process.*, *26*(4), 544–557.

Rosenberry, D. O., P. Z. Klos, and A. Neal (2012), In situ quantification of spatial and temporal variability of hyporheic exchange in static and mobile gravel-bed rivers, *Hydrol. Process.*, *26*(4), 604–612.

Schmidt, C., B. Conant Jr, M. Bayer-Raich, and M. Schirmer (2007), Evaluation and field-scale application of an analytical method to quantify groundwater discharge using mapped streambed temperatures, *J. Hydrol.*, *347*(3–4), 292–307.

Schneider, R. L., T. L. Negley, and C. Wafer (2005), Factors influencing groundwater seepage in a large, mesotrophic lake in New York, *J. Hydrol.*, *310*, 1–16.

Schuster, P. F., M. M. Reddy, J. W. LaBaugh, R. S. Parkhurst, D. O. Rosenberry, T. C. Winter, R. C. Antweiler, and W. E. Dean (2003), Characterization of lake water and ground water movement in the littoral zone of Williams Lake, a closed-basin lake in north central Minnesota, *Hydrol. Process.*, *17*, 823–838.

Sholkovitz, E., C. Herbold, and M. Charette (2003), An automated dye-dilution based seepage meter for the time-series measurement of submarine groundwater discharge, *Limnol. Oceanogr. Methods*, *1*, 16–28.

Simonds, F. W., and K. A. Sinclair (2002), Surface water-ground water interactions along the Lower Dungeness River and vertical hydraulic conductivity of streambed sediments, Clallam County, Washington, September 1999-July 2001, Water-Resour. Invest. Rep. 02–4161, 60 pp., U.S. Geol. Surv.

Simonds, F. W., P. W. Swarzenski, D. O. Rosenberry, C. D. Reich, and A. J. Paulson (2008), Estimates of nutrient loading by ground-water discharge into the Lynch Cove Area of Hood Canal, Washington, Sci. Invest. Rep. 2008–5078, 54 pp., U.S. Geol. Surv., Reston, Va.

Simpkins, W. W. (2006), A multiscale investigation of ground water flow at Clear Lake, Iowa, *Ground Water*, *44*(1), 35–46.

Smith, C. F., D. B. Chadwick, R. J. Paulsen, and J. G. Groves (2003), Development and deployment of an ultrasonic groundwater seepage meter: a reliable way to measure groundwater seepage, paper presented at Oceans 2003 Proceedings, Institute of Electrical and Electronics Engineers, San Diego, Calif., 22–26 Sept. 2003.

Stieglitz, T., M. Taniguchi, and S. Neylon (2008), Spatial variability of submarine groundwater discharge, Ubatuba, Brazil, *Est. Coast. Shelf Sci.*, *76*, 493–500.

Storey, R. G., K. W. F. Howard, and D. D. Williams (2003), Factors controlling riffle-scale hyporheic exchange flows and their seasonal changes in a gaining stream: A three-dimensional groundwater flow model, *Water Resour. Res.*, *39*(2), 1034, doi:10.1029/2002WR001367.

Swarzenski, P. W., F. W. Simonds, A. J. Paulson, S. Kruse, and C. Reich (2007), Geochemical and geophysical examination of submarine groundwater discharge and associated nutrient loading estimates into Lynch Cove, Hood Canal, WA, *Environ. Sci. Technol.*, *41*, 7022–7029.

Szilagyi, J., Z. Gribovszki, P. Kalicz, and M. Kucsara (2008), On diurnal riparian zone groundwater-level and streamflow fluctuations, *J. Hydrol.*, *349*, 1–5.

Taniguchi, M., and Y. Fukuo (1993), Continuous measurements of groundwater seepage using an automatic seepage meter, *Ground Water*, *34*(4), 675–679.

Taniguchi, M., and Y. Fukuo (1996), An effect of seiche on groundwater seepage rate into Lake Biwa, Japan, *Water Resour. Res.*, *32*(2), 333–338.

Tryon, M., K. Brown, L. Dorman, and A. Sauter (2001), A new benthic aqueous flux meter for very low to moderate discharge rates, *Deep Sea Res. I*, *48*, 2121–2146.

Turner, I. L., and G. Masselink (1998), Swash infiltration-exfiltration and sediment transport, *J. Geophys. Res.*, *103*(C13), 30,813–30,824.

U.S. Geological Survey (2013), Water-resources data for the United States, Water Year 2012, *Water-Data Rep. WDR-US-2012, site 12436000*, U.S. Geol. Surv.

White, W. N. (1932), A method of estimating ground-water supplies based on discharge by plants and evaporation from soil; results of investigations in Escalante Valley, Utah, *Water-Supply Pap. W 0659-A*, 105 pp., U.S. Geol. Surv.

Winter, T. C. (1983), The interaction of lakes with variably saturated porous media, *Water Resour. Res.*, *19*(5), 1203–1218.

Winter, T. C. (2003), Geohydrologic setting of the Cottonwood Lake area, in *Hydrological, Chemical, and Biological Characteristics of a Prairie Pothole Wetland Complex under Highly Variable Climate Conditions–The Cottonwood Lake Area, East-Central North Dakota*, edited by T. C. Winter, pp. 1–24, U.S. Geol. Surv. Prof. Pap. 1675, Denver, Colo.